United States Department of the Interior

Geological Survey

# DEPTH AND TEMPERATURE OF PERMAFROST ON THE ALASKAN ARCTIC SLOPE; PRELIMINARY RESULTS

by

Arthur H. Lachenbruch, J. H. Sass, L. A. Lawver,

Max C. Brewer, and T. H. Moses, Jr.

U.S. Geological Survey Open-File Report 82-1039

1982

## Abstract

As permafrost is defined by its temperature, the only way to determine its depth is to monitor the return to equilibrium of temperatures in boreholes that penetrate permafrost. Such measurements are under way in 25 wells on the Alaskan Arctic Slope; 21 are in Naval Petroleum Reserve Alaska (NPRA), and 4 are in the foothills to the east. Near-equilibrium results indicate that permafrost thickness in NPRA generally ranges between 200 and 400 m (compared to 600+ m at Prudhoe Bay); there are large local variations and no conspicuous regional trends. By contrast the long-term mean temperature of the ground surface (one factor determining permafrost depth) varies systematically from north to south in a pattern modified by the regional topography. The observed variation in permafrost temperature and depth cannot result primarily from effects of surface bodies of water or regional variations in heat flow; they are consistent, however, with expectable variations in the thermal conductivity of the sediments. It remains to be determined (with conductivity measurements) whether certain sites with anomalously high local gradients have anomalously high heat flow; if they do, they might indicate upwelling of interstitial fluids in the underlying basin sediments.

## INTRODUCTION

The temperature and depth of permafrost in Arctic sedimentary basins are matters of considerable importance in connection with petroleum exploration and production. They are also matters about which there is much confusion and surprisingly little information. They are important because a knowledge of the temperature field is needed for an understanding of the state of material (water, ice, brine, and gas hydrates) filling pores in the sediment, and this in turn, is important to the interpretation of seismic surveys, and to engineering problems associated with well completions and the production, storage, and transportation of petroleum. Permafrost conditions are a source of confusion largely for semantic reasons. To many investigators, "permafrost" is identified with material containing ice, and this has led to estimates of "permafrost depth" from a variety of surface and downhole geophysical measurements based on inferences of the effect of such ice on the particular property (mechanical or electrical) being measured. Although much of the interest in permafrost depends upon the presence or absence of ice, this casual usage has led to "permafrost" meaning different things to different people, depending on their method of measurement. To avoid this confusion between definition and physical inference, permafrost was initially defined by its (negative centigrade) temperature (Muller, 1947). Consequently, there is only one way to determine the depth of permafrost and that is to measure temperatures in an undisturbed borehole that penetrates it. The reason so little information is available on the temperature and depth of permafrost is that holes drilled by the petroleum industry do not generally remain idle and accessible for precision temperature logging during the long times required for the thermal disturbance caused by drilling to dissipate.

Osterkamp and Payne (1981) have recently completed a comprehensive study of 150 wells in Arctic Alaska from which they inspected well logs for indications of the maximum depth of ice-bearing sediments. The product is a useful "tentative map of the thickness of ice-bearing permafrost on the North Slope of Alaska," mostly in the region east of NPRA. They have been careful to make the distinction between "ice-bearing permafrost" and "permafrost," and they discuss the uncertainties in determining whether or not ice is present from various types of well-log data. Osterkamp and Payne conclude that in coarse-grained ice-rich material of the type characteristic of the Prudhoe Bay area, the base of ice-bearing strata can be detected from (non-thermal) logs without difficulty, but in the finer grained sediments generally found to the west on NPRA, it cannot. This is consistent with our findings from the two areas. In any case, however, a knowledge of undisturbed temperature at the base of ice-bearing sediments is necessary for an understanding of the physical conditions controlling the occurrence of the ice.

A rare opportunity to obtain undisturbed temperatures in permafrost was provided through the efforts of George Gryc and his associates in the Office of National Petroleum Reserve - Alaska (NPRA). During the course of exploratory drilling on NPRA, 21 of the wells were completed according to a special procedure in which the upper 600 m were filled with a non-freezing fluid (diesel oil) and preserved in a condition that permits subsequent re-entry for precision temperature logging. Through the courtesy of the Mobil, Exxon, BP, Sinclair, and Forest Oil Companies, four other wells on the Alaskan North Slope were preserved for our use in a similar condition. We have relogged these 25 wells (some several times) and many are now close to thermal equilibrium. In this interim report, we present a brief summary of results of these observations along with some similar results from a few other North

Slope wells. A more complete report analyzing thermal conductivity and heat flow will be presented after all of the wells have had sufficient time for their drilling disturbance to dissipate to the point where their undisturbed temperatures can be estimated with confidence. We have recently completed a more comprehensive study (like that planned for NPRA) of permafrost conditions near Prudhoe Bay (Lachenbruch and others, 1982); some results from that study are compared to our new information from NPRA in this report.

## PRESENTATION OF THE DATA (TABLE 1)

Some basic information from each of the 25 holes observed in this study is summarized in table 1. The locations of the holes are shown in figure 1;

---

TABLE 1 and Figure 1 near here

---

21 are in Naval Petroleum Reserve Alaska, and 4 are in the foothills of the Brooks Range to the east. All of the holes were completed without a surface plug and with the portion of the casing in permafrost filled with diesel oil to prevent re-freezing. This makes it possible for us to relog them at convenient intervals to trace the dissipation of the drilling disturbance and the re-establishment of natural formation temperatures. Temperature measurements were made at depth intervals of 5-10 m with a multiconductor cable and thermistor thermometer (the "portable mode" described by Sass and others, 1971). The number of logs made in each hole to date is shown in column (b) of table 1.

A sample of the data is shown in figure 2 for the site at Atigaru Point

---

Figure 2 near here

---

(ATI) on the coast at Harrison Bay (fig. 1). The duration of the drilling disturbance (i.e., of the period between the start of drilling and the final cessation of circulation) is denoted by s. For the example in figure 2, s was 65 days; for the other holes, the value of s is given in column (a) of table 1.

It is well known that the dissipation of the drilling disturbance depends on the ratio of the time elapsed since completion of the disturbance, t*, to

the duration of the disturbance, s. We denote this "dimensionless time" by $\tau$, i.e.,

$$\tau = t^*/s \qquad (1)$$

For the five successive logs illustrated in figure 2, $\tau$ ranged from 4.2 to 25 which represents observations made from 273 days to 1625 days (4½ years) after completion of drilling. The value of $\tau$ for the last observation in each hole is given in column (c), table 1.

For observations that are not taken too soon after the completion of drilling (i.e., for sufficiently large $\tau$), the temperature at any depth in a drill hole is usually given to a good approximation by assuming that drilling acted as a constant heat source of duration s. This assumption leads to the expectation that successive temperature measurements at a given depth will be given by (Lachenbruch and Brewer, 1959).

$$\theta(\tau) \cong A \, \ell n\left(1 + \frac{1}{\tau}\right) + \theta_\infty \qquad (2)$$

where $\theta(\tau)$ is the temperature observed at dimensionless time $\tau$, $\theta_\infty$ is the undisturbed pre-drilling temperature, and A is a constant. Thus after an initial period (depending on the departure of the actual drilling process from the constant-source model) a straight line of slope A is expected in a plot of borehole temperature versus $\ell n\ (1 + 1/\tau)$; extrapolation to $\ell n\ (1 + 1/\tau) = 0$ (i.e., to $\tau = \infty$) yields an estimate of $\theta_\infty$. Such a plot for ATI is shown in figure 2b for depth increments of 100 m. Extrapolation of the empirically determined straight line to the right-hand margin of figure 2b shows that the observed temperatures were about 0.2°C above the undisturbed temperatures $\theta_\infty$ at the time of the last observation. We refer to this disturbance as $\Delta\theta$; an estimate for each of the holes is given in column (d) of table 1. The dots plotted in figure 2a represent the estimated equilibrium temperatures obtained from figure 2b.

A second example of the observations is given in figure 3 for Lisburne

---

Figure 3 near here

---

(LBN) which lies in the foothills near the southern boundary of NPRA (fig. 1). At this site, the drilling operation lasted almost a year (s = 357 days), the value of $\tau$ at the last observation was only 1.25, and we have only two logs, making it impossible to confirm the straight line used for extrapolation to $\theta_\infty$. An additional problem results from the fact that there was a 63-day hiatus in drilling between an initial period lasting 73 days ($s_1$) and a final period lasting 221 days ($s_2$). The hiatus can be accounted for by treating the disturbance as the effect of two successive drilling operations. Letting t** be the time elapsed since the conclusion of the first stage of drilling, we define two dimensionless times

$$\tau_1 = t^{**}/s_1$$

$$\tau_2 = t^{*}/s_2$$

and apply equation (2) twice to obtain

$$\theta = A\{\ell n(1 + \frac{1}{\tau_1}) + \ell n(1 + \frac{1}{\tau_2})\} + \theta_\infty \qquad (3)$$

Figure 3b is a plot of observed temperature against the quantity in braces in equation (3). Linear extrapolation to the right-hand margin yields an estimate of equilibrium temperatures which are shown for 50-m depth intervals and plotted as the squares in figure 3a. Accounting for the drilling hiatus with equation (3) increases our confidence in the extrapolation to $\theta_\infty$, and it illustrates a simple means of refining equation (2). It can be shown, however, that in the present case the refinement has little effect on the

result, a testimony to the robust nature of equation (2). In spite of the large drilling disturbance ($\Delta\theta \sim 1.7°C$) at the time of the last observation, we believe that the estimated values for $\theta_\infty$ are correct to within a few tenths °C.

Linear extrapolation of the equilibrium temperatures (dots, fig. 2a, squares, fig. 3a) to the surface z = 0, yields an estimate of the long-term mean annual temperature to which the present deep permafrost temperatures have adjusted. We denote this quantity by $\theta_o$; for ATI (fig. 2a) it is about -10.8°C; for LBN (fig 3a) it is about -5.9°C. Estimates of $\theta_o$ for the other holes can be found in column (e), table 1. It is seen from the curvature in the upper 100 m at ATI (fig. 2a) that the complete profile extrapolates to a surface temperature warmer than $\theta_o$; the discrepancy represents a climatic warming of the last century (see e.g., Lachenbruch and others, 1982). The data from LBN (fig. 3) are too far from equilibrium to determine whether the climatic anomaly occurs there.

By definition, permafrost extends to the depth at which the undisturbed formation temperature is 0°C. This depth denoted by z*, is estimated from figure 2 to be 402 m at ATI, and for LBN it is 285 m (fig. 3). Estimates of permafrost depths for the other holes are given in column (f), table 1. The average equilibrium thermal gradient in permafrost is denoted by $\Gamma^*$ and given by

$$\Gamma^* = -\theta_o/z^* \qquad (4)$$

where $\theta_o$ is measured in °C. $\Gamma^*$ is tabulated for each hole in column (g), table 1.

Although all permafrost is below 0°C, only part of the permafrost can contain ice because the freezing temperature of pore water is generally depressed below 0°C by the confining pressure, dissolved salts, and (in fine-grained materials) by capillary forces (see e.g., Osterkamp and Payne, 1981).

However, interstitial ice-like structures can be formed by hydrates of natural gas which may be stable under conditions that extend below the base of permafrost (e.g., Katz, 1971). Where appreciable amounts of ice are present in permafrost, its presence can often be detected by the tendency of its latent heat of refreezing to retard the dissipation of the drilling disturbance (see e.g., Lachenbruch and others, 1982). Thus the separation of the early temperature profiles (curves: $\tau$ = 4.2, 8.4, and 14) in figure 2a suggests that the bottom of an ice-rich layer occurs at a depth of about 330 m. Estimates of depths to the bottoms of ice-rich layers for some of the other holes are tabulated in column (h), table 1.

## PERMAFROST TEMPERATURES AND GAS HYDRATE STABILITY

Figure 4 is a composite plot of temperatures observed in holes on the

---

Figure 4 near here

---

coastal plane in NPRA. We have excluded the three coastal plane holes (TLK, IKP, and KUY) for which the average drilling disturbance ($\Delta\theta$, table 1) was estimated to exceed 0.7°C at the time of the last observation. Their profiles would fall within the envelope of those shown, but they are irregular and would complicate an already congested illustration. Shown also in figure 4 is the envelope of near-equilibrium profiles from nine holes on the coastal plane near Prudhoe Bay (from Lachenbruch and others, 1982).

A similar composite graph is shown for holes in the foothills of the Brooks Range in figure 5. (We have taken the boundary between the foothills

---

Figure 5 near here

---

and coastal plane as the 50-m elevation contour, roughly consistent with the classification of Wahrhaftig (1965).) The profiles from Umiat and Awuna (SBE and AWU, table 1) were excluded, as they were far from equilibrium and quite irregular. For LBN, which is also far from equilibrium but more regular, we have included the equilibrium temperatures estimated in figure 3; they are represented by the squares in figure 5.

The dashed arcuate curve in figures 4 and 5 represents the phase boundary for stability of methane hydrate in the presence of pure water (from Katz, 1971) on the assumption that the confining pressure is hydrostatic. Below and to the left of the curve, solid ice-like methane hydrate could occur; above it

and to the right, it could not. Increasing salinity of the pore water would shift the curve downward; decreasing the molecular weight of the gas would move it upward. If the confining pressure were increased from the assumed hydrostatic values (those caused by an overburden with unit specific gravity) to lithostatic values (those caused by the full overburden weight of the sediments) the curve would be shifted upward to about half the depth shown. At any locality gas hydrates are possible only where the thermal profile lies below the appropriate phase boundary curve. According to Kharaka and Carothers (1982), in the Barrow area the hydrostatic assumption is approximately correct and the compensating effects of salinity and gas composition lead to a stability curve close to the one shown in figures 4 and 5. Under these conditions, gas hydrates could occur to depths ~500 m at the colder sites on the coastal plane (e.g., JWD, ATI, and ESN, fig. 4) and at the warmer sites, there could be none. Similarly at some of the foothill sites it could occur to depths ~600 m (e.g., LBN and LUP, fig. 5). At the Prudhoe Bay sites, the temperatures are much lower (dashed envelope, figs. 4 and 5) and according to Kharaka and Carothers (1982) the phase boundary curve is shifted ~10°C to the right by the gas composition there. It is seen that under these circumstances, if gas hydrates occur at Prudhoe Bay, they can be stable to great depths.

## REGIONAL VARIATIONS

Rewriting equation (4), we can consider the depth of permafrost $z^*$ to be controlled by two factors, the long-term mean surface temperature $\theta_o$ and the mean thermal gradient $\Gamma^*$, i.e.,

$$z^* = \frac{-\theta_o}{\Gamma^*} \qquad (5)$$

Low (i.e., large negative) values of surface temperature $\theta_o$, and small thermal gradients $\Gamma^*$ favor deep permafrost (large $z^*$). Our best estimates of $\theta_o$ are shown adjacent to the hole designations in figure 1. The designations enclosed in parentheses represent five wells (not included in table 1) from which earlier observations were available: SB3 (S. Barrow No. 3, Lachenbruch and Brewer, 1959), S28 (Simpson No. 28, Brewer, 1958), CTD (Cape Thompson Hole D, Lachenbruch and others, 1966) and UM9 and TP1 (Umiat 9 and Togoruk No. 1, Brewer, unpublished). The rectangular boundary south of Prudhoe Bay (fig. 1) encloses the sites studied by Lachenbruch and others (1982). The generalized contours in figure 1 show that the estimated values of $\theta_o$ vary systematically, increasing from north to south in a pattern modified by the regional topography. This is not surprising as $\theta_o$ is controlled by climate which is known also to vary according to this pattern. (Local topography in the Brooks Range will, of course, cause extreme local departures from the pattern.) From equation 5, we should expect the permafrost depth $z^*$ also to follow this simple regional pattern if the mean thermal gradient in permafrost $\Gamma^*$ were relatively uniform from place to place.

That this is not the case is best seen from figure 6 in which the

---

Figure 6 near here

---

equilibrium depth to permafrost z* is plotted against long-term mean annual surface temperature $\theta_o$. The vertical dashed line at $\theta_o$ = -9°C separates data obtained in the coastal plane from those obtained in the foothills. Although the foothills generally have higher surface temperatures, the mean permafrost thickness for our (9-well) sample there (300 m ±13 m standard error) is not significantly different than the mean for the (19-well) sample from the coastal plane (314 m ± 14 m standard error excluding Prudhoe Bay). The diagonal lines in figure 6, which represent constant values of mean permafrost gradient $\Gamma^*$, illustrate how lower gradients at the foothill sites generally compensate for higher surface temperatures to maintain substantial permafrost thicknesses there. Even within the thin coastal band north of the contour $\theta_o$ = -12°C (fig. 1), permafrost thickness undergoes extreme local variations (from 280 m at Simpson 28 to 420 m at JWD, right-hand side of fig. 6). More generally, it is seen from figure 6 and figure 1 that in NPRA, permafrost thickness varies by a factor of about 2 (from 200 m to 400+ m) and, unlike $\theta_o$, its variation shows no conspicuous regional trends on the scale of our sample. The anomalously deep permafrost at Prudhoe Bay is illustrated by the rectangle in figure 6.

## REASONS FOR LOCALLY VARYING PERMAFROST DEPTH

We have seen that the permafrost depth undergoes local variations unrelated to the regional trend in mean surface temperature. There are three possible reasons for this: 1) local effects of bodies of water on temperatures at the solid-earth surface, 2) lateral variations in heat flow from below permafrost, and 3) lateral variations in the thermal conductivity of permafrost. It is premature to undertake a detailed discussion of these factors, as studies of sediment conductivity, equilibrium temperatures of permafrost, and thermal gradients at depth, which are in progress will provide a great deal of relevant information. We shall present only a brief outline of the problem.

### Effects of bodies of water

The wells from which we have measured temperatures are all on "dry" land where, as we have seen, the mean surface temperature on the coastal plane is ∿-10°C. However, some sites are within a few hundred meters of the ocean shoreline and many are close to lakes, which in some parts of the coastal plane, cover 30%-50% of the surface. Those portions of lakes and seas deeper than ∿2 m do not freeze to the bottom, and consequently they have mean bottom temperatures close to 0°C (slightly higher for fresh water; slightly lower for salt water; see Lachenbruch and others, 1962). Thus the solid surface on the coastal plane undergoes local changes in mean temperature from ∿0° to ∿-10°; we have sampled only emergent sites, and they are presently at the cold end of this range. However, the shorelines of bodies of water in permafrost are continually migrating. Some of our sites were, in the past, beneath deep lakes and accordingly had surface temperatures ∿10°C warmer than they do today. It is seen from the coastal plane profiles in figure 4 that the range of temperatures at depths of a few hundred meters is of the order of 10°C. If

we had no information other than that in figure 4, we might contrive histories of migrating lakes that could account for this range of temperatures. For example, the warmer profiles in figure 4 require that the 10°C surface anomaly propagate to depths ~500 m; this would require a large deep lake over the site for several tens of thousands of years; subsequent drainage over the last few thousand years would have to be postulated to account for the low temperatures observed at shallower depths. From temperature observations made at depths of a few kilometers in these wells, however, we know that the temperature differences among wells persist, and in fact increase, at depth (Blanchard and Tailleur, oral communication). To account for these temperature differences at such great depths with surface bodies of water is quite impossible; they would have to persist for millions of years. There is little doubt that surface bodies of water can have substantial effects on permafrost temperature (e.g., Lachenbruch and others, 1966), that some of the differences among the profiles in figure 4 result from this cause, and that detailed studies of such differences might yield useful geomorphic information. However, the major cause of the local variability in permafrost depth that we have observed must be controlled by other factors.

## Thermal conductivity and heat flow

It has been shown that the local variability of permafrost depth results from local variability in the mean thermal gradient $\Gamma^*$ in permafrost. For the reasonable assumption of one-dimensional steady-state conductive heat flow in permafrost, $\Gamma^*$ can be expressed

$$\Gamma^* = q/k \qquad (6)$$

where k is the (harmonic) mean thermal conductivity of the permafrost section and q is the rate at which heat enters its base (per unit area). Local variations in either q or k can cause variable $\Gamma^*$.

Figure 7 (modified from Lachenbruch and others, 1982) shows how thermal

---

Figure 7 near here

---

conductivity of a saturated sediment varies with the mean thermal conductivity of its grains ($k_g$) and porosity $\phi$ for the case where the pores are filled with ice (solid curves) or water (dashed curves). For quartz-rich silicic sediments the grain conductivities are in the range 10-14 mcal/cm sec °C (upper three solid or dashed curves, fig. 7), for argillaceous grains they are in the range 4-6 mcal/cm sec °C, and for coal they are typically $\lesssim 2$ mcal/cm sec °C. We have measured mean grain conductivities that cover this complete range in samples of drill cuttings from wells in northern Alaska. The porosities ($\phi$, fig. 7) of these sediments typically lie in the range 20%-50%. Coarse-grained sediments in permafrost often have most of their moisture frozen, fine-grained sediments often do not. Figure 6 shows that on the coastal plane $\Gamma^*$ varies by a factor of about 2; within individual profiles, the gradient varies with depth by a factor of about 3. Inspection of figure 7 and equation 6 leaves little doubt that these local variations in gradient can be easily explained by the expectable ranges of $k_g$ and $\phi$. It will be noted that the tendency toward lower gradients $\Gamma^*$ in the foothills (fig. 6) is consistent with a uniform regional heat flow q (equation 6), and the occurrence of higher conductivities as expected in the more competent rocks of the foothills.

Whether or not heat flow (q, equation 6) varies across northern Alaska cannot be addressed until thermal conductivity studies are completed from some of the wells in which gradients have been measured. It is clear from the discussion of conductivity, however, that no heat-flow variation is required by the available observations. If the heat flow from depth is not augmented

by vertically moving fluids, its lateral changes would be very gradual and could not explain the local variations observed. It remains to be seen whether sites with anomalously high local gradients such as South Meade and N. Kalikpuk have anomalously high heat flow; if they do, they might indicate an upwelling of interstitial fluids in the underlying basin sediments.

Acknowledgment. We are grateful to David Blanchard and Irvin Tailleur for discussions of their unpublished tabluations of temperatures obtained at great depths in some of the NPRA holes. We also thank Reuben Kachadoorian for helpful review of our manuscript, and Fred Grubb and Peter Galanis for their assistance in obtaining some of the temperature data upon which this work is based.

## References cited


Brewer, M. C., 1958, Some results of geothermal investigations of permafrost in northern Alaska: Transactions, American Geophysical Union, v. 39, p. 19-26.

Katz, D. L., 1971, Depths to which frozen gas fields (gas hydrates) may be expected: Journal of Petroleum Technology, v. 23, p. 419-423.

Kharaka, Y. K., and Carothers, W. W., 1982, Geochemistry of oil-field waters from North Slope, Alaska: this volume.

Lachenbruch, A. H., and Brewer, M. C., 1959, Dissipation of the temperature effect of drilling a well in Arctic Alaska: U.S. Geological Survey Bulletin 1083-C, p. 73-109.

Lachenbruch, A. H., Brewer, M. C., Greene, G. W., and Marshall, B. V., 1962, Temperatures in permafrost, in Temperature--Its Measurement and Control in Science and Industry, v. 3, part 1: New York, Reinhold, p. 791-803.

Lachenbruch, A. H., Greene, G. W., and Marshall, B. V., 1966, Permafrost and the geothermal regimes, in Wilimovsky, N. J., and Wolfe, J. N., eds., Environment of the Cape Thompson Region, Alaska: U.S. Atomic Energy Commission, Division of Technical Information, p. 149-163.

Lachenbruch, A. H., Sass, J. H., Marshall, B. V., and Moses, T. H., Jr., 1982, Permafrost, heat flow, and the geothermal regime at Prudhoe Bay, Alaska: Journal of Geophysical Research, in press.

Muller, S. W., 1947, Permafrost, or permanently frozen ground, and related engineering problems: U.S. Engineers Office, Strategic Eng. Study Special Rept. 62, 136 p.

Osterkamp, T. E., and Payne, M. W., 1981, Estimates of permafrost thickness from well logs in northern Alaska: Cold Regions Science and Technology, v. 5, p. 13-27.

Sass, J. H., Lachenbruch, A. H., Munroe, R. J., Greene, G. W., and Moses, T. H., Jr., 1971, Heat flow in the western United States: Journal of Geophysical Research, v. 76, p. 6376-6413.

Wahrhaftig, Clyde, 1965, Physiographic divisions of Alaska: U.S. Geological Survey Professional Paper 482, 52 p.

TABLE 1. Permafrost data from wells on the Alaskan Arctic Slope

| Hole designation | Abbrev. | N. Lat. | W. Long. | Elev. (m) | (a) Drilling duration s (days) | (b) No. of logs | (c) last log $\tau$ | (d) last log $\Delta\theta$ (°C) | (e) equilibrium condition $\theta_o$ (extrap.) (°C) | (f) equilibrium condition pf depth $z^*$ (m) | (g) equilibrium condition pf grad. $\Gamma^*$ (°C/km) | (h) Bottom, ice-rich layer (m) |
|---|---|---|---|---|---|---|---|---|---|---|---|---|
| E. Teshekpuk | ETK | 70.57° | 152.94° | 2 | 60 | 3 | 20 | 0.1 | -10.8 | 252 | 43 | |
| S. Harrison Bay | SOH | 70.42° | 151.73° | 7 | 79 | 5 | 21 | 0.3 | -11.5 | 375†† | 31 | |
| Atigaru Point | ATI | 70.55° | 151.72° | 2 | 65 | 5 | 25 | 0.2 | -10.8 | 402 | 27 | 330 |
| Fish Creek #1 | FCK | 70.32° | 152.06° | 28 | 72 | 5 | 22 | 0.3 | -11.0 | 260 | 42 | 140 |
| Drew Point | DRP | 70.87° | 153.89° | 4 | 59 | 3 | 21 | 0.2 | -11.0 | 320 | 34 | 250 |
| N. Kalikpuk | NKP | 70.51° | 152.37° | 6 | 46 | 4 | 27 | 0.2 | -11.1 | 210 | 53 | 180? |
| S. Meade | SME | 70.61° | 156.89° | 12 | 349 | 3 | 2.7 | 0.7 | - 9.9 | 205 | 48 | 160 |
| Kugrua | KAG | 70.59° | 158.66° | 20 | 106 | 4 | 11 | 0.3 | -10.4 | 282 | 37 | |
| Tunalik | TLK | 70.20° | 161.07° | 26 | 423 | 2 | 1.4 | 2.0 | - 9.8 | 285 | 34 | |
| Peard Bay | PEA | 70.71° | 159.00° | 23 | 76 | 3 | 11 | 0.4 | -10.2 | 310 | 33 | |
| Ikpikpuk | IKP | 70.45° | 154.33° | 10 | 458 | 2 | 1.2 | 1.0 | -10 | 340 | 29 | 280? |
| E. Simpson #1 | ESN | 70.92° | 154.62° | 4 | 50 | 3 | 17 | 0.4 | -10.9 | 370 | 30 | 280 |
| J. W. Dalton | JWD | 70.92° | 153.14° | 6 | 86 | 3 | 8.8 | 0.5 | -12.0 | 420 | 29 | 310? |
| Lisburne | LBN | 68.48° | 155.68° | 556 | 357 | 2 | 1.2 | 1.7 | - 5.9 | 285 | 21 | |
| Seabee | SBE | 69.37° | 152.17° | 89 | 289 | 2 | 1.8 | 1.4 | - 8.6 | 310 | 28 | 210 |
| W. Dease | WDS | 71.15° | 155.62° | 2 | 36 | 2 | 14.3 | 0.4 | -12.0 | 300 | 40 | |
| S. Barrow 16 | SBW | 71.28° | 156.54° | 4 | 20 | 4 | 64 | 0.1 | | | | |
| †Exxon Canning River | CNR | 69.60° | 146.36° | 282 | 107 | 4 | 24 | 0.2 | - 8.3 | 282 | 29 | |
| †Mobile Echooka | E81 | 69.40° | 147.27° | 200 | 160 | 3 | 20 | 0.2 | - 6.2 | 280 | 22 | 260 |
| †Sinclair/BP Kuparik #1 | KK1 | 69.30° | 150.81° | 190 | 207 | 1 | 6.2 | 0.5 | - 8.4 | 300 | 28 | |
| †Forest Oil Lipine #1 | LUP | 69.10° | 148.62° | 524 | 309 | 3 | 7.5 | 0.4 | - 4.6 | 240 | 19 | |
| Koluktuk | KOL | 69.75° | 154.61° | 56 | 23 | 1 | 5.7 | 0.5 | - 8.4 | 290†† | 29 | |
| Awuna | AWU | 69.15° | 158.02° | | 411 | 1 | 0.31 | 2.0 | | | | |
| Tulageak | TUL | 71.19° | 155.73° | 3 | 21 | 1 | 7.5 | 0.5 | -12 | 310 | 39 | |
| Kuyanak | KUY | 70.26° | 156.06° | 3 | 41 | 1 | 3.7 | 0.8 | -10.3 | 320 | 32 | |

†Outside of NPRA.

††Extrapolated value.

## Illustrations

Figure 1. Map of northern Alaska showing well locations (dots), generalized contours of long-term mean surface temperature $\theta_o$ (°C), and the value of $\theta_o$ for each well. Data from the five wells with designations in parentheses are from previous studies.

Figure 2a. Successive temperature profiles from the well at Atigaru Point observed from 271 days ($\tau$ = 4.17) to 1625 days ($\tau$ = 25) after completion of drilling. Dots represent estimates of undisturbed temperature.

2b. Representation of the dissipation of the drilling disturbance (equation 2) for selected depths shown in right-hand margin. $\tau$ is time elapsed since completion of drilling measured in multiples of the drilling periods (s = 65 days).

Figure 3a. Temperature profiles from LBN taken 100 days ($\tau$ = .28) and 714 days ($\tau$ = 2.0) after completion of drilling. Squares represent estimates of undisturbed temperature.

3b. Representation of the dissipation of the drilling disturbance (equation 3) for selected depths indicated in right-hand margin. $\tau$ is post-drilling time measured in multiples of the time elapsed from start-up to final completion s (= 357 days); $\tau_1$ is dimensionless time since completion of first stage of drilling of duration $s_1$ (= 73 days), $\tau_2$ is dimensionless time since completion of second stage of drilling of duration $s_2$ (= 221 days).

Figure 4. Latest temperature profiles from wells in NPRA on the Coastal Plain (see table 1). Dashed curves enclose region occupied by similar profiles from the Prudhoe Bay area (Lachenbruch and others, 1982). Arcuate (dash-dot) curve is phase boundary for Methane Hydrate (see text).

Figure 5. Latest temperature profiles from wells in foothills of Brooks Range (see table 1). Squares represent estimated equilibrium temperatures for LBN (from fig. 3). Dashed curves enclose region occupied by similar profiles from the Prudhoe Bay area (Lachenbruch and others, 1982). Arcuate (dash-dot) curve is phase boundary for Methane Hydrate (see text).

Figure 6. Plot of estimated permafrost depth $z^*$ versus long-term mean surface temperature $\theta_o$ for North Slope wells. Rectangle encloses results from wells near Prudhoe Bay (Lachenbruch and others, 1982). Well designations in parentheses indicate data obtained from previous studies. Vertical dashed line separates wells on Coastal Plain from those in foothills. Diagonal lines join points of equal mean permafrost gradient $\Gamma^*$.

Figure 7. Chart for estimating thermal conductivity of saturated sediment with mean grain conductivity $k_g$ and porosity $\phi$; solid curves are for pores containing ice; dashed curves are for pores containing water (modified from Lachenbruch and others, 1982).

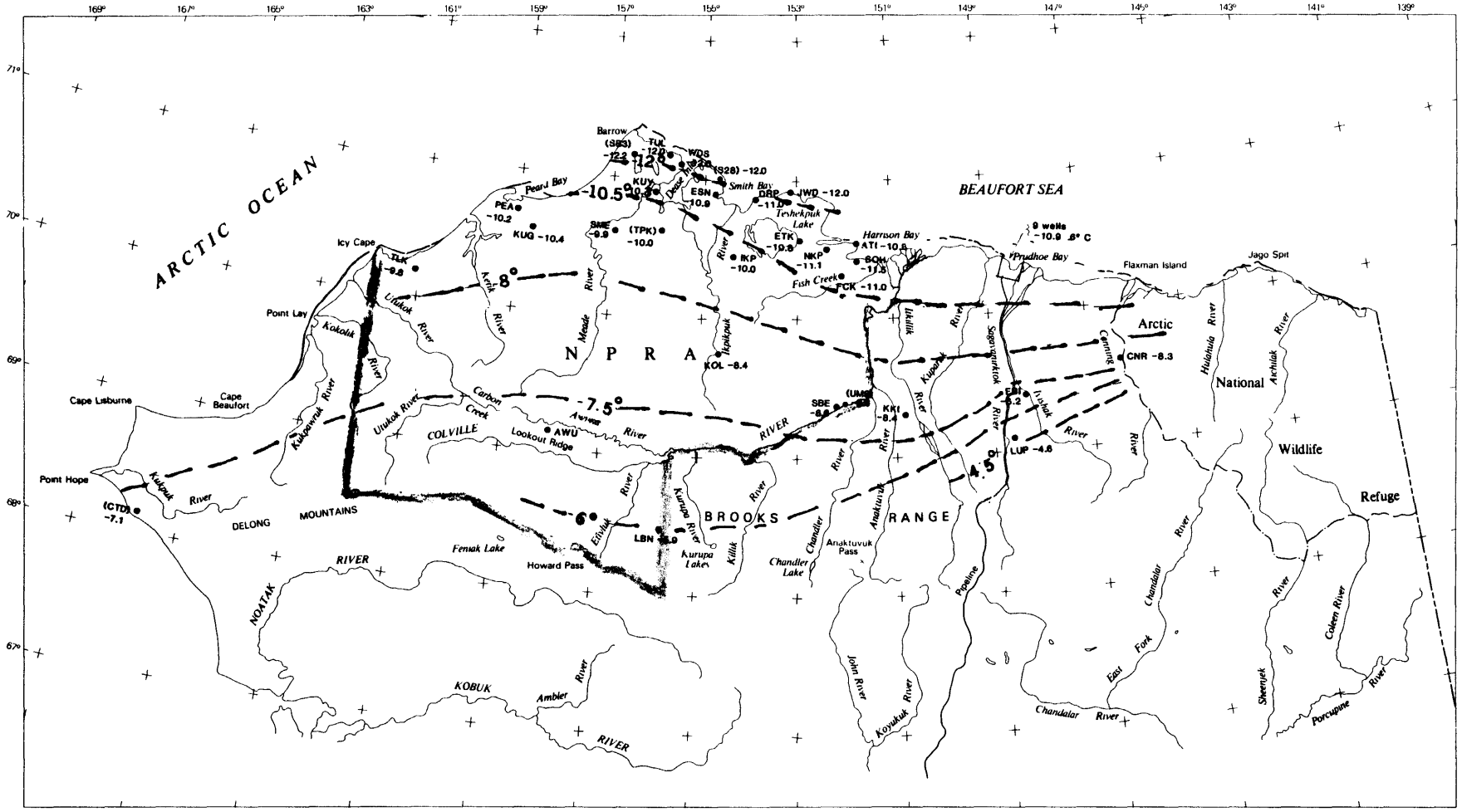


Figure 1. Map of northern Alaska showing well locations (dots), generalized contours of long-term mean surface temperature $\theta_o$ (°C), and the value of $\theta_o$ for each well. Data from the five wells with designations in parentheses are from previous studies.

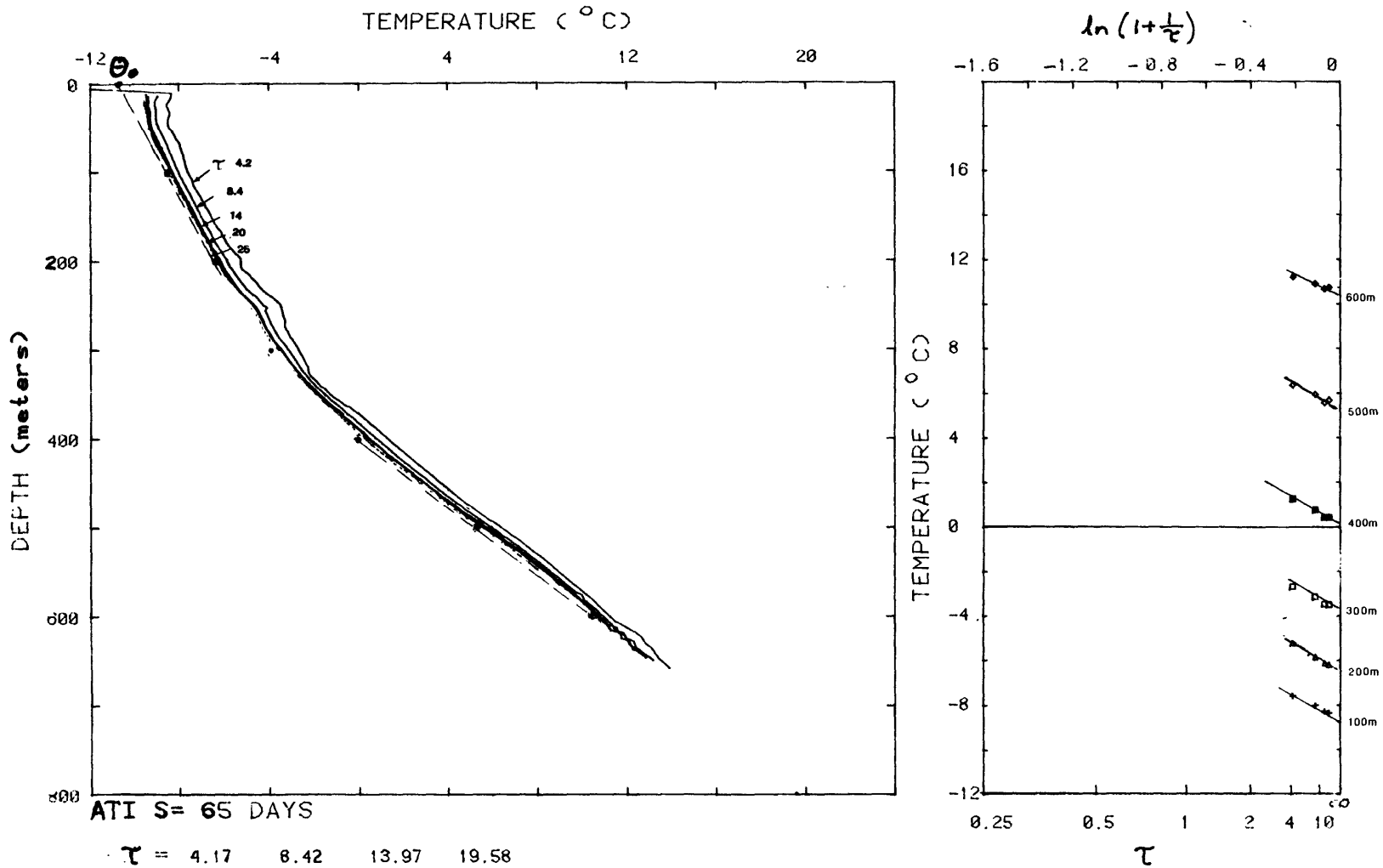


Figure 2a. Successive temperature profiles from the well at Atigaru Point observed from 271 days (τ = 4.17) to 1625 days (τ = 25) after completion of drilling. Dots represent estimates of undisturbed temperature.

2b. Representation of the dissipation of the drilling disturbance (equation 2) for selected depths shown in right-hand margin. τ is time elapsed since completion of drilling measured in multiples of the drilling period (s = 65 days).

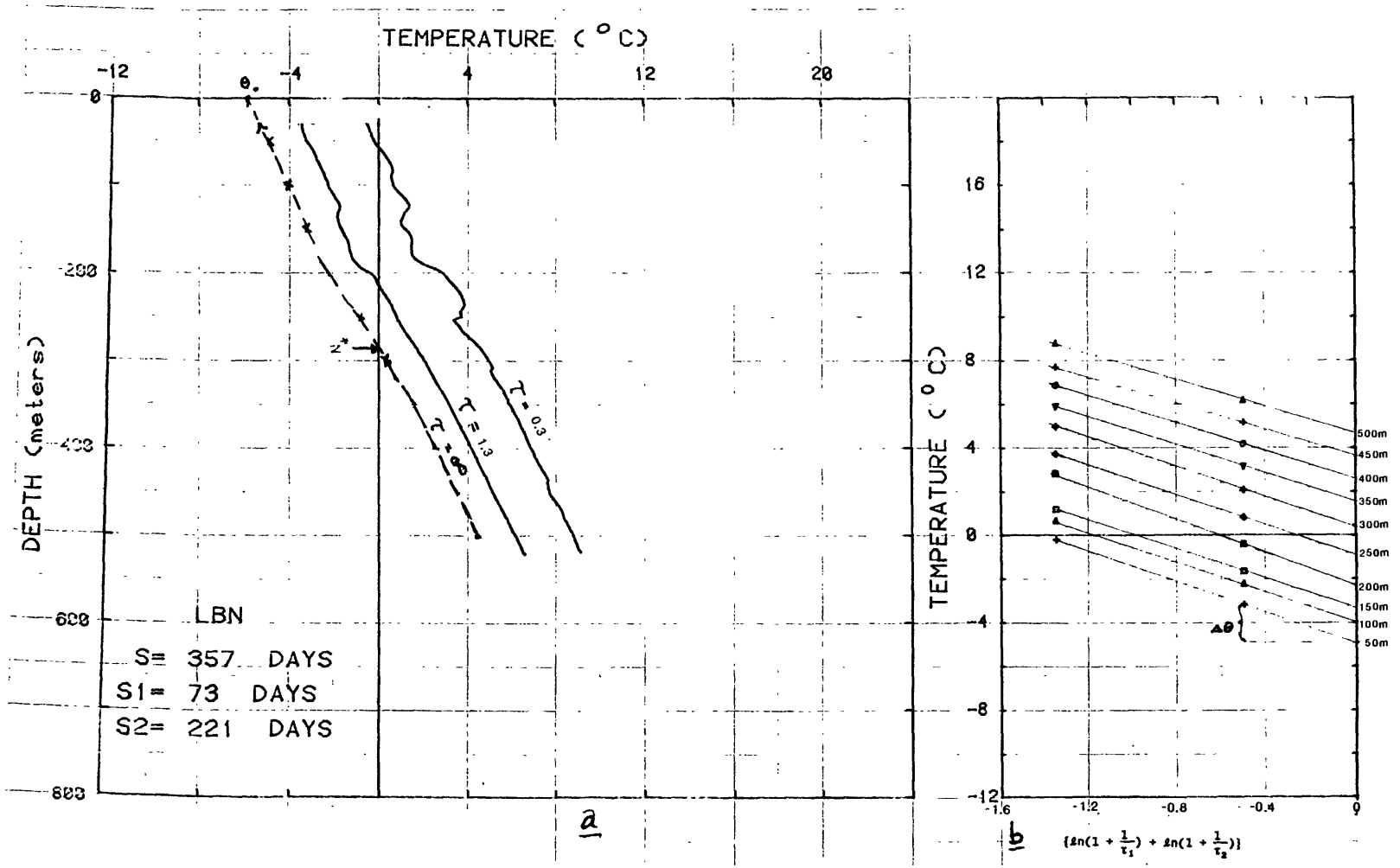


Figure 3a. Temperature profiles from LBN taken 100 days ($\tau$ = .28) and 714 days ($\tau$ = 2.0) after completion of drilling. +'s represent estimates of undisturbed temperature.

3b. Representation of the dissipation of the drilling disturbance (equation 3) for selected depths indicated in right-hand margin. $\tau$ is post-drilling time measured in multiples of the time elapsed from start-up to final completion s (= 357 days); $\tau_1$ is dimensionless time since completion of first stage of drilling of duration $s_1$ (= 73 days), $\tau_2$ is dimensionless time since completion of second stage of drilling of duration $s_2$ (= 221 days).

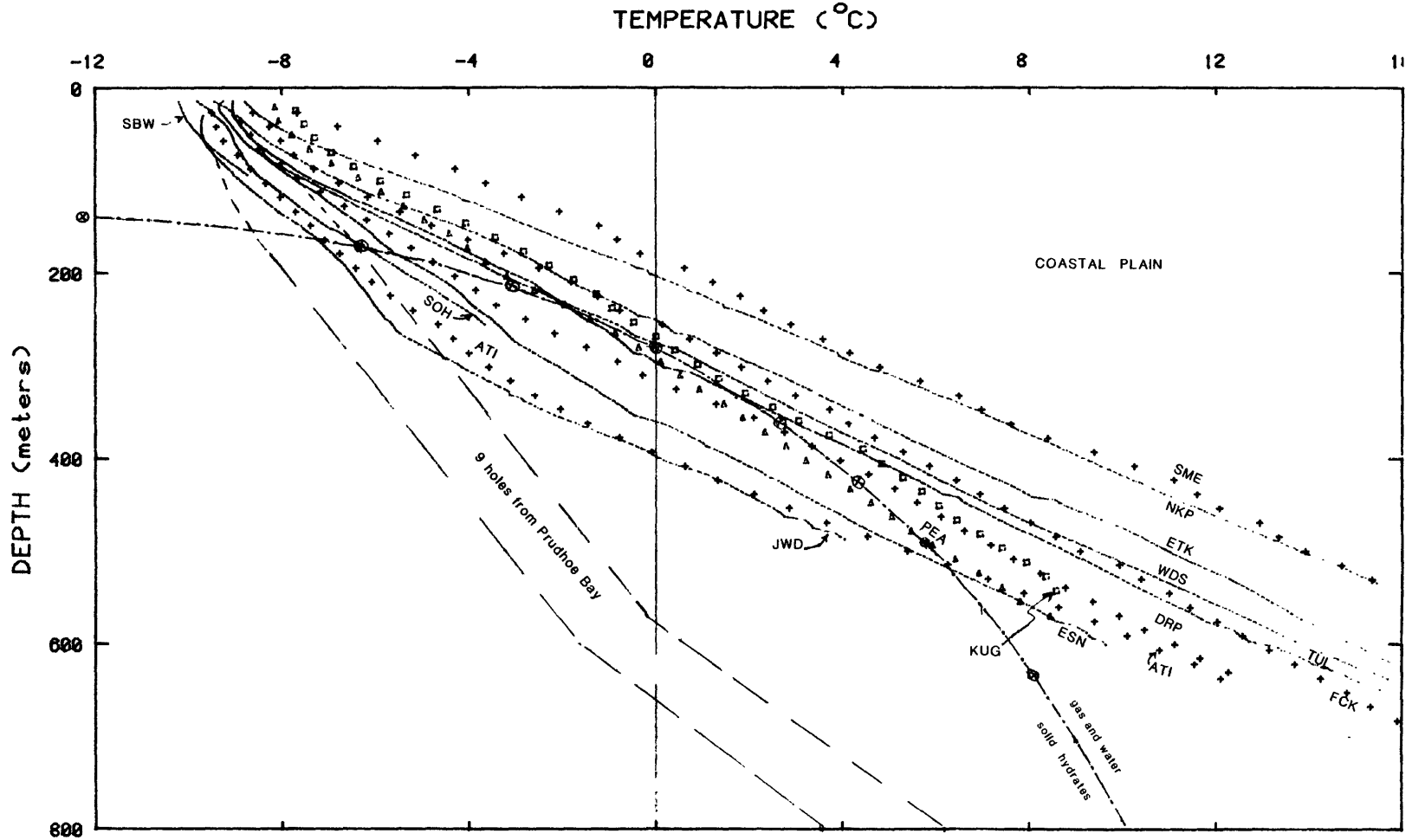


Figure 4. Latest temperature profiles from wells in NPRA on the Coastal Plain (see table 1). Dashed curves enclose region occupied by similar profiles from the Prudhoe Bay area (Lachenbruch and others, 1982). Arcuate (dash-dot) curve is phase boundary for Methane Hydrate (see text).

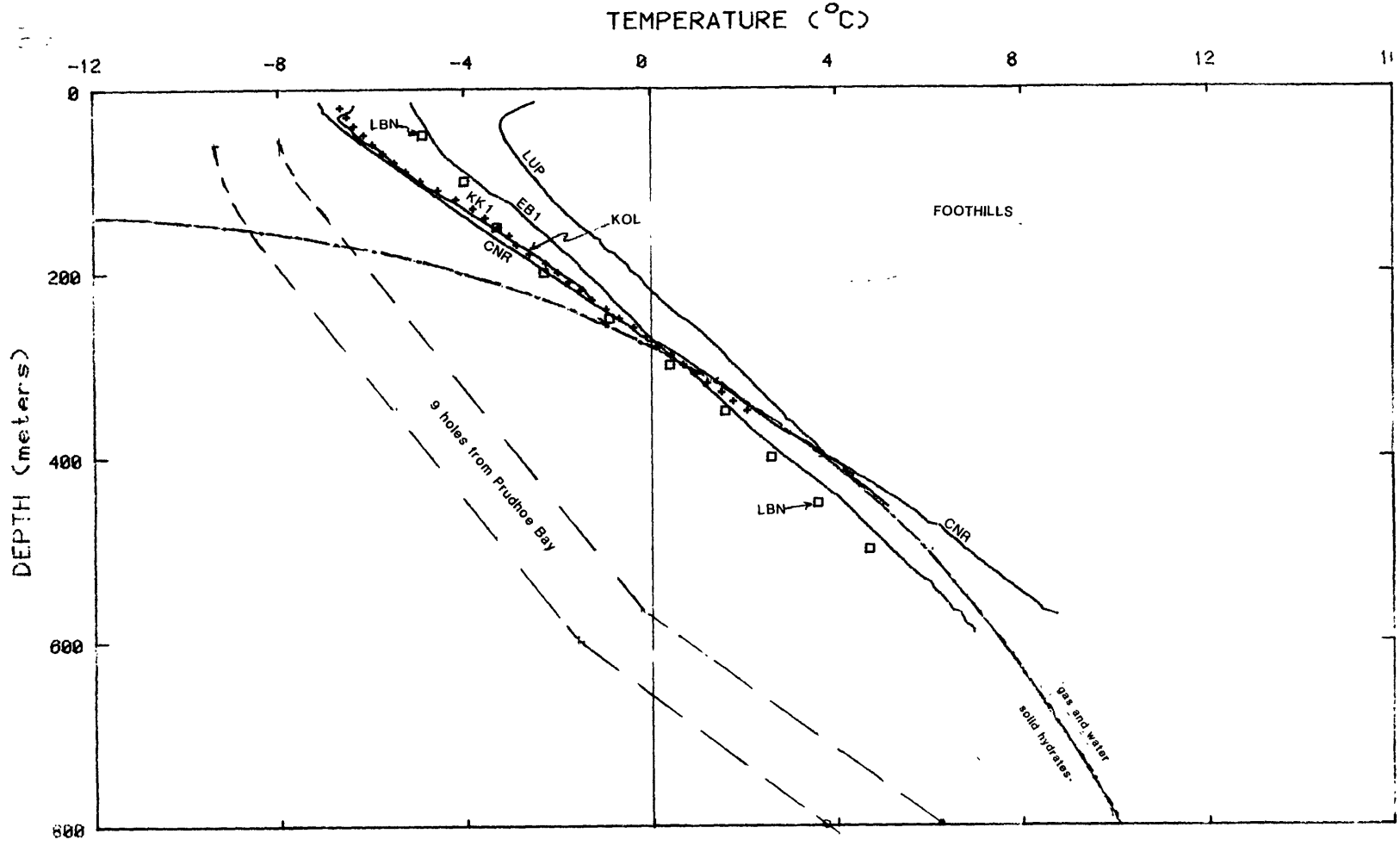


Figure 5. Latest temperature profiles from wells in foothills of Brooks Range (see table 1). Squares represent estimated equilibrium temperatures for LBN (from fig. 3). Dashed curves enclose region occupied by similar profiles from the Prudhoe Bay area (Lachenbruch and others, 1982). Arcuate (dash-dot) curve is phase boundary for Methane Hydrate (see text).

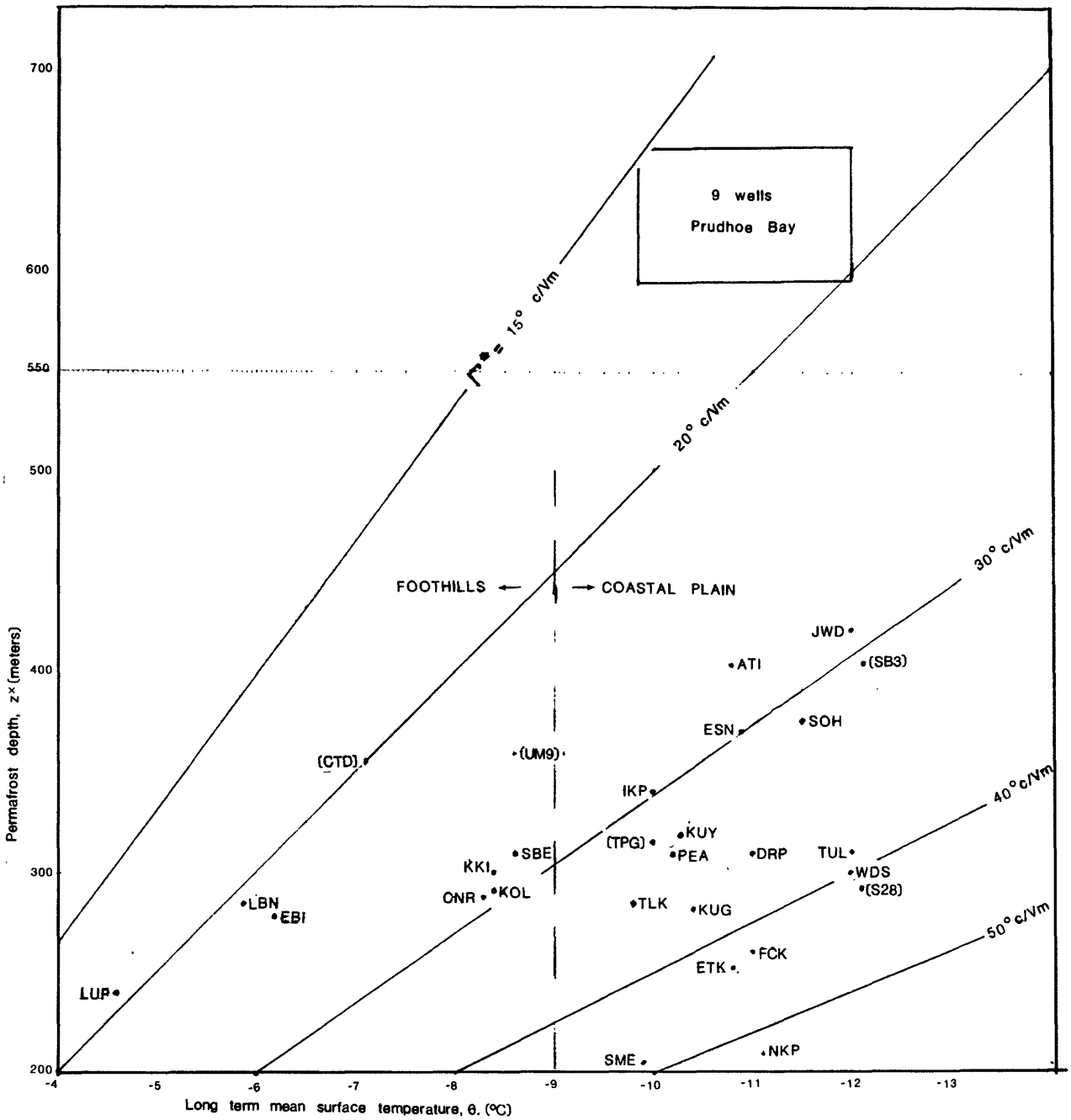


Figure 6. Plot of estimated permafrost depth z* versus long-term mean surface temperature $\theta_o$ for North Slope wells. Rectangle encloses results from wells near Prudhoe Bay (Lachenbruch and others, 1982). Well designations in parentheses indicate data obtained from previous studies. Vertical dashed line separates wells on Coastal Plain from those in foothills. Diagonal lines join points of equal mean permafrost gradient $\Gamma^*$.

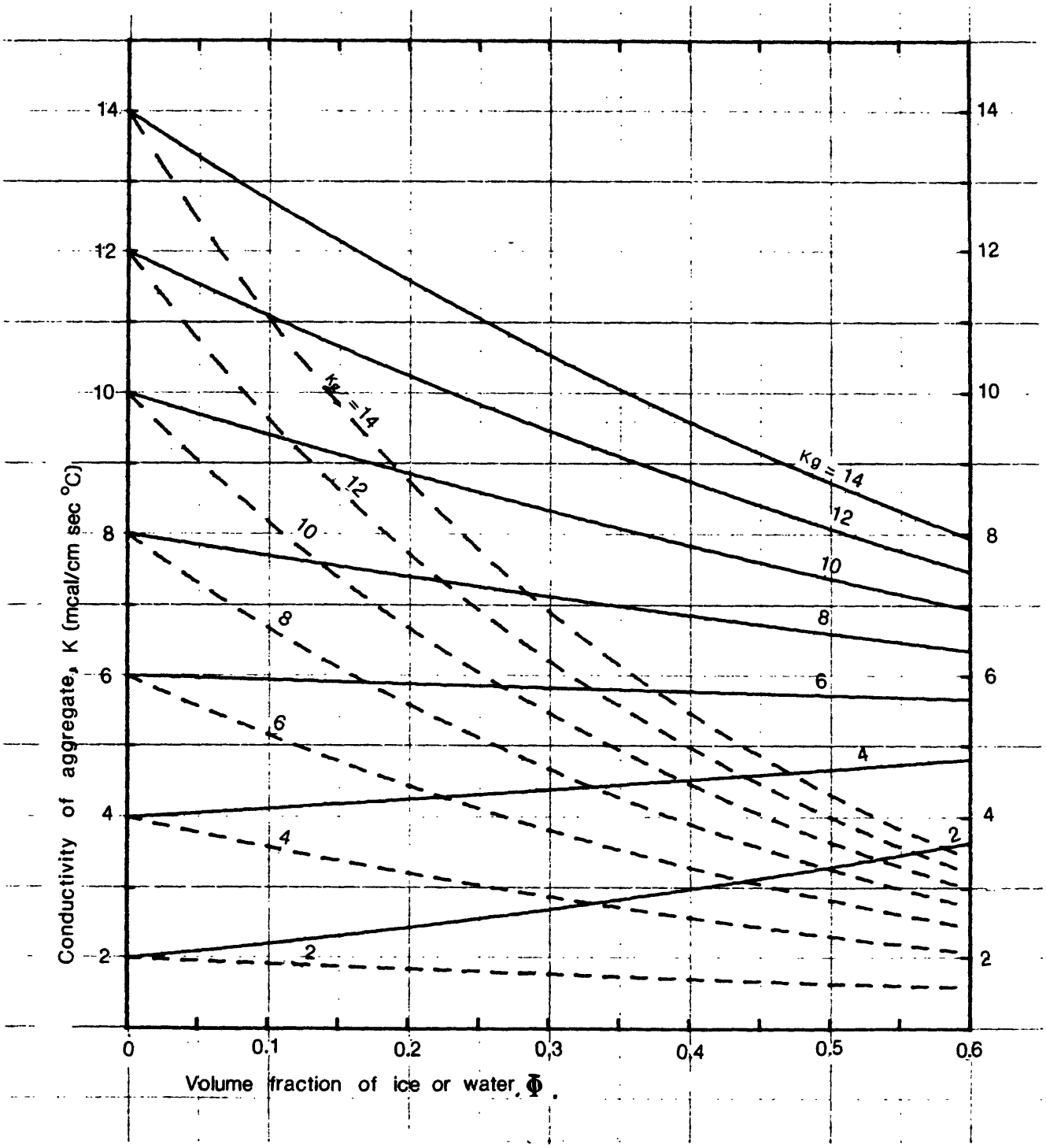


Figure 7. Chart for estimating thermal conductivity of saturated sediment with mean grain conductivity $k_g$ and porosity $\phi$; solid curves are for pores containing ice; dashed curves are for pores containing water (modified from Lachenbruch and others, 1982).